



e-ISSN: 2319-8753 | p-ISSN: 2347-6710

IJRSET

International Journal of Innovative Research in
SCIENCE | ENGINEERING | TECHNOLOGY



INTERNATIONAL JOURNAL OF INNOVATIVE RESEARCH

IN SCIENCE | ENGINEERING | TECHNOLOGY

Volume 12, Issue 12, December 2023

ISSN INTERNATIONAL
STANDARD
SERIAL
NUMBER
INDIA

Impact Factor: 8.423

9940 572 462

6381 907 438

ijirset@gmail.com

www.ijirset.com

Spectral and Thermal Analysis of Ho³⁺ ions doped Ytterbium Zinc Lithium Potassium Calcium Alumino Borophosphate Glasses

S.L. Meena

Ceramic Laboratory, Department of physics, Jai Narain Vyas University, Jodhpur (Raj.) India

E-mail address:shankardiya7@rediffmail.com

ABSTRACT: Glasses samples containing Ho³⁺ in ytterbium zinc lithium potassium calcium alumino borophosphate glasses (25-x)P₂O₅: 10ZnO: 10Li₂O: 10K₂O: 10CaO: 10Al₂O₃:10Yb₂O₃:15B₂O₃:xHo₂O₃. (where x=1, 1.5,2 mol %) have been prepared by melt-quenching method. The amorphous nature of the prepared glass samples was confirmed by X-ray diffraction. Optical absorption, Excitation and fluorescence spectra were recorded at room temperature for all glass samples. Judd-Ofelt intensity parameters Ω_{λ} ($\lambda=2, 4$ and 6) are evaluated from the intensities of various absorption bands of optical absorption spectra. Using these intensity parameters various radiative properties like spontaneous emission probability (A), branching ratio (β), radiative life time (τ_R) and stimulated emission cross-section (σ_p) of various emission lines have been evaluated.

KEYWORDS: YZLPCABP Glasses, Optical Properties, Thermal Properties, Judd-Ofelt Theory,

I. INTRODUCTION

Glasses doped with rare earth ions have drawn much attention due to their potential applications in optical amplifier, optical fibers, sensors, glass lasers, up-conversion lasers, electro-luminescent devices solid state lasers, optical sensors and fluorescence labeling [1-6]. Oxide glasses are the most stable host matrices for practical applications due to their high chemical durability and thermal stability. The importance of glasses doped with rare earth elements lies in their distinctive emission and laser properties in several electromagnetic spectral regions [7-10]. Glasses containing phosphate oxide glasses have wide range application in the field of glass ceramics, electronic device, thermal and mechanical sensors, reflecting windows [11-13]. Due to their excellent thermal, physical, optical and mechanical properties, they are used in fiber lasers, optical devices thermal imaging, spectral conversion, memory devices, energy production, ultrafast optical switches, photonic devices and infrared transmission components [14-15]. Zinc oxide is added in the glass matrix to increase glass forming ability and stability in the glass system. Among active rare-earth ions Ho³⁺ exhibits high solubility in ceramic glasses, which also possess excellent Thermal, physical and optical properties [16-20].

The present work reports on the preparation and characterization of rare earth doped heavy metal oxide (HMO) glass systems for lasing materials. I have studied on the Optical absorption, Excitation, fluorescence spectra of Ho³⁺ doped ytterbium zinc lithium potassium calcium alumino borophosphate glasses. The intensities of the transitions for the rare earth ions have been estimated successfully using the Judd-Ofelt theory, The laser parameters such as radiative probabilities (A), branching ratio (β), radiative life time (τ_R) and stimulated emission cross section (σ_p) are evaluated using J.O. intensity parameters (Ω_{λ} , $\lambda=2,4$ and 6).

II. EXPERIMENTAL TECHNIQUES

Preparation of glasses

The following Ho³⁺ doped borophosphate glass samples (25-x)P₂O₅: 10ZnO: 10Li₂O: 10K₂O: 10CaO: 10Al₂O₃:10Yb₂O₃:15B₂O₃: x Ho₂O₃. (where x=1,1.5 and 2 mol%) have been prepared by melt-quenching method. Analytical reagent grade chemical used in the present study consist of P₂O₅, ZnO, Li₂O, K₂O, CaO, Al₂O₃: Yb₂O₃, B₂O₃ and Ho₂O₃. They were thoroughly mixed by using an agate pestle mortar. then melted at 1065^oC by an electrical muffle furnace for 2h., After complete melting, the melts were quickly poured in to a preheated stainless steel mould and annealed at temperature of 250^oC for 2h to remove thermal strains and stresses. Every time fine powder of cerium

oxide was used for polishing the samples. The glass samples so prepared were of good optical quality and were transparent. The chemical compositions of the glasses with the name of samples are summarized in **Table 1**.

Table 1.

Chemical composition of the glasses

Sample	Glass composition (mol %)
YZLPCABP (UD)	25P ₂ O ₅ : 10ZnO: 10Li ₂ O: 10K ₂ O: 10CaO: 10Al ₂ O ₃ :10Yb ₂ O ₃ :15B ₂ O ₃
YZLPCABP (HO1)	24P ₂ O ₅ : 10ZnO: 10Li ₂ O: 10K ₂ O: 10CaO: 10Al ₂ O ₃ :10Yb ₂ O ₃ :15B ₂ O ₃ :1 Ho ₂ O ₃
YZLPCABP (HO1.5)	23.5P ₂ O ₅ : 10ZnO: 10Li ₂ O: 10K ₂ O: 10CaO: 10Al ₂ O ₃ :10Yb ₂ O ₃ :15B ₂ O ₃ :1.5 Ho ₂ O ₃
YZLPCABP (HO2)	23P ₂ O ₅ : 10ZnO: 10Li ₂ O: 10K ₂ O: 10CaO: 10Al ₂ O ₃ :10Yb ₂ O ₃ :15B ₂ O ₃ :2 Ho ₂ O ₃
YZLPCABP (UD)	-Represents ytterbium zinc lithium potassium calcium alumino borophosphate glass specimen.
YZLPCABP (HO)	-Represents Ho ³⁺ doped ytterbium zinc lithium potassium calcium alumino borophosphate glass specimens

III. THEORY

3.1 Oscillator Strength

The intensity of spectral lines are expressed in terms of oscillator strengths using the relation [21].

$$f_{\text{expt.}} = 4.318 \times 10^{-9} \int \epsilon(\nu) d\nu \quad (1)$$

where, $\epsilon(\nu)$ is molar absorption coefficient at a given energy ν (cm⁻¹), to be evaluated from Beer–Lambert law.

Under Gaussian Approximation, using Beer–Lambert law, the observed oscillator strengths of the absorption bands have been experimentally calculated [22], using the modified relation:

$$P_m = 4.6 \times 10^{-9} \times \frac{1}{cl} \log \frac{I_0}{I} \times \Delta\nu_{1/2} \quad (2)$$

where c is the molar concentration of the absorbing ion per unit volume, l is the optical path length, $\log I_0/I$ is optical density and $\Delta\nu_{1/2}$ is half band width.

3.2. Judd-Ofelt Intensity Parameters

According to Judd [23] and Ofelt [24] theory, independently derived expression for the oscillator strength of the induced forced electric dipole transitions between an initial J manifold $|4f^N(S, L) J\rangle$ level and the terminal J' manifold $|4f^N(S', L') J'\rangle$ is given by:

$$\frac{8\pi^2 mc\nu}{3h(2J+1)n} \frac{1}{n} \left[\frac{(n^2+2)^2}{9} \right] \times S(J, J') \quad (3)$$

Where, the line strength $S(J, J')$ is given by the equation

$$S(J, J') = e^2 \sum_{\lambda=2, 4, 6} \Omega_{\lambda} \langle 4f^N(S, L) J || U^{(\lambda)} || 4f^N(S', L') J' \rangle^2 \quad (4)$$

In the above equation m is the mass of an electron, c is the velocity of light, ν is the wave number of the transition, h is Planck's constant, n is the refractive index, J and J' are the total angular momentum of the initial and final level respectively, Ω_{λ} ($\lambda=2, 4$ and 6) are known as Judd-Ofelt intensity.

3.3 Radiative Properties

The Ω_{λ} parameters obtained using the absorption spectral results have been used to predict radiative properties such as spontaneous emission probability (A) and radiative life time (τ_R), and laser parameters like fluorescence branching ratio (β_R) and stimulated emission cross section (σ_p).

The spontaneous emission probability from initial manifold $|4f^N(S', L') J'\rangle$ to a final manifold $|4f^N(S, L) J\rangle$ is given by:

$$A [(S', L') J'; (S, L) J] = \frac{64 \pi^2 v^3}{3h(2J'+1)} \left[\frac{n(n^2+2)^2}{9} \right] \times S(J', \bar{J}) \tag{5}$$

Where, $S(J', J) = e^2 [\Omega_2 \|U^{(2)}\|^2 + \Omega_4 \|U^{(4)}\|^2 + \Omega_6 \|U^{(6)}\|^2]$

The fluorescence branching ratio for the transitions originating from a specific initial manifold $|4f^N(S', L') J' \rangle$ to a final many fold $|4f^N(S, L) J \rangle$ is given by

$$\beta [(S', L') J'; (S, L) J] = \sum_{S L J} \frac{A[(S' L)]}{A[(S' L') J'(\bar{S} L)]} \tag{6}$$

where, the sum is over all terminal manifolds.

The radiative life time is given by

$$\tau_{rad} = \sum_{S L J} A[(S', L') J'; (S, L) J] = A_{Total}^{-1} \tag{7}$$

where, the sum is over all possible terminal manifolds. The stimulated emission cross-section for a transition from an initial manifold $|4f^N(S', L') J' \rangle$ to a final manifold $|4f^N(S, L) J \rangle$ is expressed as

$$\sigma_p(\lambda_p) = \left[\frac{\lambda_p^4}{8\pi c n^2 \Delta\lambda_{eff}} \right] \times A[(S', L') J'; (\bar{S}, \bar{L}) \bar{J}] \tag{8}$$

where, λ_p the peak fluorescence wavelength of the emission band and $\Delta\lambda_{eff}$ is the effective fluorescence line width.

3.4 Nephelauxetic Ratio (β') and Bonding Parameter ($b^{1/2}$)

The nature of the R-O bond is known by the Nephelauxetic Ratio (β') and Bonding Parameters ($b^{1/2}$), which are computed by using following formulae [25, 26]. The Nephelauxetic Ratio is given by

$$\beta' = \frac{v_g}{v_a} \tag{9}$$

where, v_a and v_g refer to the energies of the corresponding transition in the glass and free ion, respectively. The value of bonding parameter ($b^{1/2}$) is given by

$$b^{1/2} = \left[\frac{1-\beta'}{2} \right]^{1/2} \tag{10}$$

IV. RESULT AND DISCUSSION

4.1 XRD Measurement

Figure 1 presents the XRD pattern of the sample contain P_2O_5 which is show no sharp Bragg's peak, but only a broad diffuse hump around low angle region. This is the clear indication of amorphous nature within the resolution limit of XRD instrument.

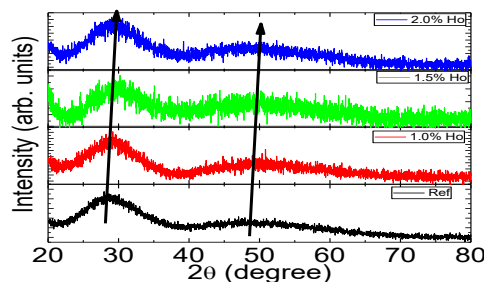


Fig. 1 X-ray diffraction pattern of YZLPCABP (HO) Glasses.

4.2 Thermal Properties

Differential thermal analysis checks the heat absorbed or evolved by glass samples during heating or cooling. Fig. 2 depicts the DTA thermogram of powdered YZLPCABP sample. The glass transition temperature (T_g), onset crystallization temperature (T_c), crystallization temperature (T_p), melting temperature (T_m), thermal stability (T_s), thermal stability parameter (S), Hurbe’s criterion (H_r) and reduced glass transition temperature (T_{rg}) were calculated. All the determined thermal parameters are given in table 2.

Glass samples	T_g (°C)	T_c (°C)	T_p (°C)	T_m (°C)	T_s (°C)	H_r (°C)	S(°C)	T_{rg} (°C)
YZLPCABP HO(01)	372	505	545	682	133	0.226	14.30	0.545
YZLPCABP HO(01)	374	507	547	685	133	0.225	14.23	0.545
YZLPCABP HO(01)	377	509	550	688	132	0.229	14.36	0.548

$$\text{Thermal stability } (T_s) = T_c - T_g \tag{11}$$

$$\text{Hruby’s criterion } (H_r) = [(T_p - T_c) / (T_m - T_c)] \tag{12}$$

$$\text{Reduced glass transition temperature } (T_{rg}) = T_g / T_m \tag{13}$$

$$\text{Thermal stability parameter } (S) = [(T_p - T_c) \times (T_c - T_g)] / T_g \tag{14}$$

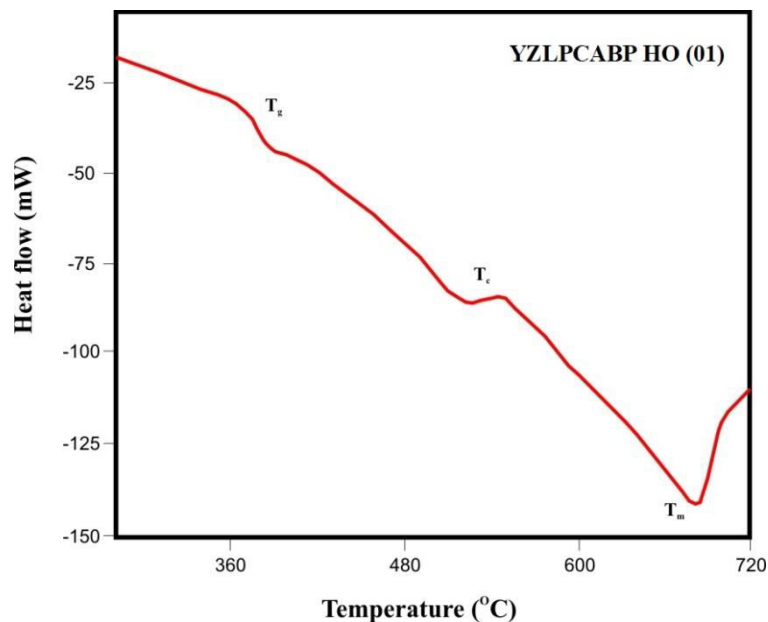


Fig. 2. DTA Curve of YZLPCABP HO (01) sample.

4.3 Absorption Spectrum

The absorption spectra of Ho^{3+} doped YZLPCABP glass specimens have been presented in Figure 3 in terms of optical density versus wavelength. Twelve absorption bands have been observed from the ground state 5I_8 to excited states 5I_5 , 5I_4 , 5F_5 , 5F_4 , 5F_3 , 3K_8 , 5G_6 , ($^5G_3, ^5G_5$), 5G_4 , 5G_2 , 5G_3 , and 3F_4 for Ho^{3+} doped YZLPCABP glasses.

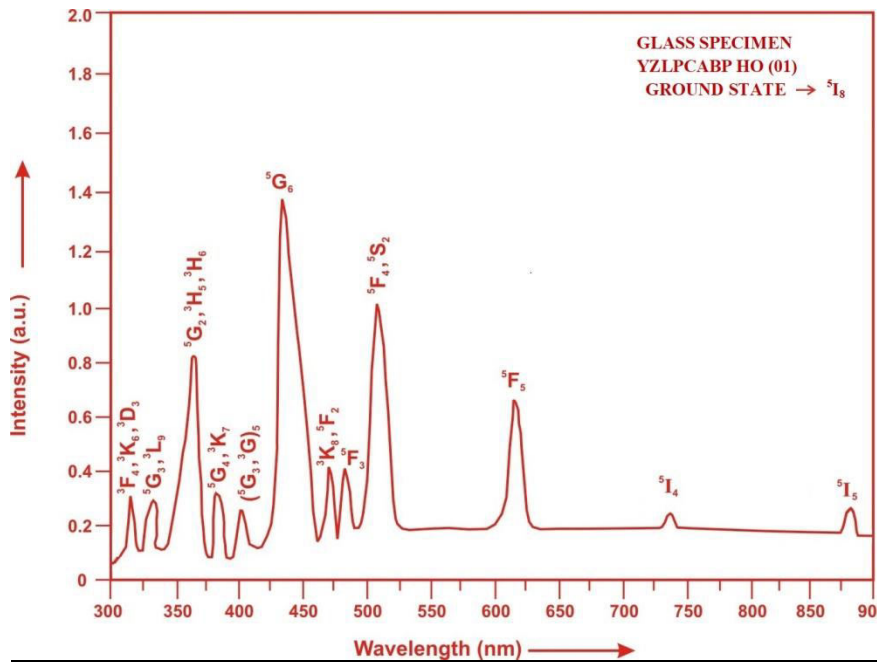


Fig. (3) Absorption spectrum of YZLPCABP HO (01) glass.

The experimental and calculated oscillator strength for Ho³⁺ ions in YZLPCABP glasses are given in **Table 3**.

Table 3: Measured and calculated oscillator strength ($P_m \times 10^{+6}$) of Ho³⁺ ions in YZLPCABP glasses.

Energy level from 5I_8	Glass YZLPCABP (HO 01)		Glass YZLPCABP (HO1.5)		Glass YZLPCABP (HO02)	
	P_{exp}	P_{cal}	P_{exp}	P_{cal}	P_{exp}	P_{cal}
5I_5	0.50	0.25	0.49	0.25	0.46	0.24
5I_4	0.07	0.02	0.06	0.02	0.05	0.02
5F_5	3.75	2.85	3.72	2.82	3.68	2.80
5F_4	4.78	4.44	4.75	4.40	4.71	4.36
5F_3	1.68	2.47	1.65	2.45	1.62	2.43
3K_8	1.48	2.03	1.45	2.00	1.41	1.98
5G_6	26.55	26.50	25.35	25.31	24.65	24.63
$(^5G_3, ^3G_5)$	3.9	1.71	3.87	1.68	3.83	1.67
5G_4	0.009	0.63	0.08	0.62	0.07	0.61
5G_2	5.98	5.62	5.93	5.41	5.89	5.28
5G_3	1.58	1.44	1.54	1.41	1.50	1.39
3F_4	1.42	4.23	1.38	4.16	1.35	4.12
r.m.s. deviation	1.1190		± 1.1120		± 1.1173	

Computed values of F_2 , Lande' parameter (ξ_{4f}), Nephelauxetic ratio (β') and bonding parameter ($b^{1/2}$) for Ho³⁺ ions in YZLPCABP glass specimen are given in Table 4.

Table 4: F_2 , ξ_{4f} , β' and $b^{1/2}$ parameters for Holmium doped glass specimen.

Glass Specimen	F_2	ξ_{4f}	β'	$b^{1/2}$
Ho ³⁺	358.82	1258.16	0.9337	0.1821

In the ytterbium zinc lithium potassium calcium alumino borophosphate glasses (YZLPCABP) Ω_2 , Ω_4 and Ω_6 parameters decrease with the increase of x from 1 to 2 mol%. The order of magnitude of Judd-Ofelt intensity parameters is $\Omega_2 > \Omega_6 > \Omega_4$ for all the glass specimens. The spectroscopic quality factor (Ω_4 / Ω_6) related with the rigidity of the glass system has been found to lie between 0.595 and 0.601 in the present glasses. The values of Judd-Ofelt intensity parameters are given in **Table 5**.

Table 5: Judd-Ofelt intensity parameters for Ho³⁺ doped YZLPCABP glass specimens.

Glass Specimen	$\Omega_2(\text{pm}^2)$	$\Omega_4(\text{pm}^2)$	$\Omega_6(\text{pm}^2)$	Ω_4 / Ω_6
YZLPCABP (HO 01)	6.509	1.356	2.256	0.6011
YZLPCABP (HO1.5)	6.169	1.332	2.237	0.5954
YZLPCABP (HO 02)	5.973	1.319	2.218	0.5947

4.4 Excitation Spectrum

The Excitation spectrum of YZLPCABP (HO 01) glass has been presented in Figure 4 in terms of Excitation Intensity versus wavelength. The excitation spectrum was recorded in the spectral region 325–525 nm fluorescence at 545nm having different excitation band centered at 349,419, 452, 473and 486 nm are attributed to the ⁵G₃, (⁵G, ³G)₅, ⁵G₆, ³K₈ and ⁵F₃ transitions, respectively. The highest absorption level is ⁵G₆ and is at 452nm. So this is to be chosen for excitation wavelength.

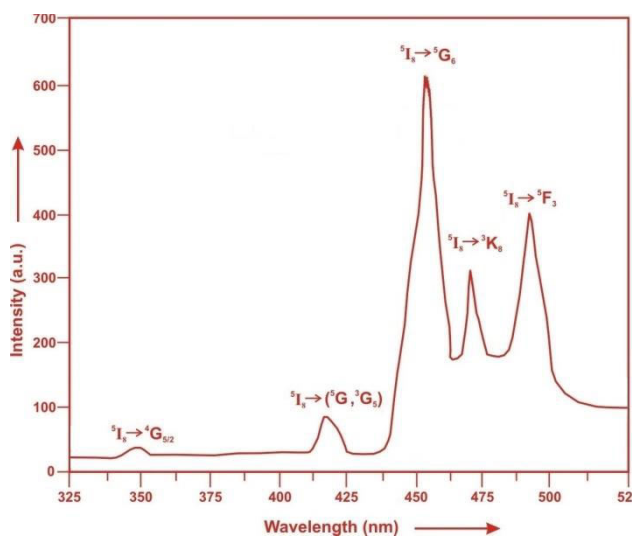


Fig. (4) Excitation spectrum of YZLPCABP HO (01) glass.

4.5 Fluorescence Spectrum

The fluorescence spectrum of Ho³⁺ doped in ytterbium zinc lithium potassium calcium alumino borophosphate glass is shown in Figure 5. There are eleven broad bands observed in the Fluorescence spectrum of Ho³⁺ doped ytterbium zinc lithium potassium calcium alumino borophosphate glass. The wavelengths of these bands along with their assignments are given in Table 6. The peak with maximum emission intensity appears at 2035 nm and corresponds to the (⁵I₇ → ⁵I₈) transition.

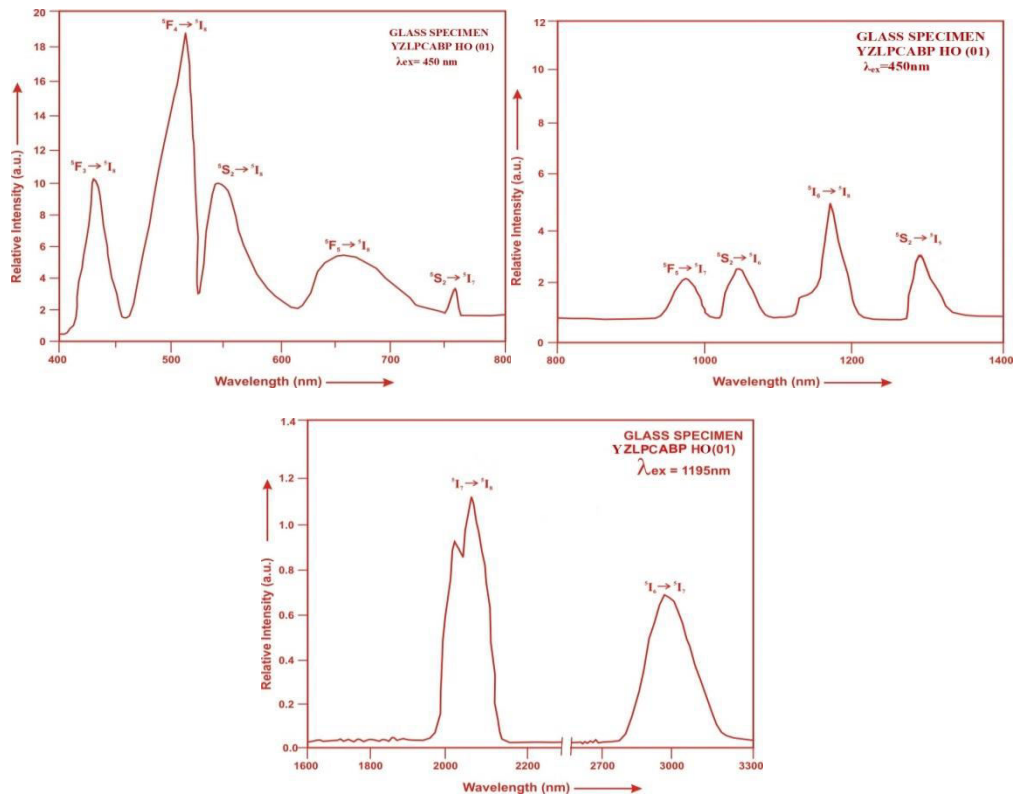


Fig. (5). Fluorescence spectrum of YZLPCABP HO (01) glass.

Table6: Emission peak wave lengths (λ_p),radiative transition probability (A_{rad}),branching ratio (β),stimulated emission cross-section(σ_p) and radiative life time(τ_R) for various transitions in Ho³⁺ doped YZLPCABP glasses.

Transition	YZLPCABP (HO 01)					YZLPCABP (HO 1.5)				YZLPCABP (HO 02)			
	λ_{max} (nm)	$A_{rad}(s^{-1})$	β	$\sigma_p (10^{-20} cm^2)$	$\tau_R(\mu s)$	$A_{rad}(s^{-1})$	β	$\sigma_p (10^{-20} cm^2)$	$\tau_R (\mu s)$	$A_{rad}(s^{-1})$	β	$\sigma_p (10^{-20} cm^2)$	$\tau_R (10^{-20} cm^2)$
$^5F_3 \rightarrow ^5I_8$	435	4317.97	0.2487	0.622	5758.77	4290.12	0.2489	0.607	5801.10	4262.13	0.2490	0.587	5841.38
$^5F_4 \rightarrow ^5I_8$	501	6835.02	0.3936	1.273		6786.51	0.3937	1.238		6737.06	0.3935	1.206	
$^5S_2 \rightarrow ^5I_8$	555	1802.38	0.1037	0.451		1790.75	0.1039	0.442		1779.07	0.1039	0.432	
$^5F_5 \rightarrow ^5I_8$	652	1950.47	0.1123	0.753		1931.38	0.1120	0.739		1918.91	0.1121	0.726	
$^5S_2 \rightarrow ^5I_7$	761	1372.74	0.0791	1.155		1363.89	0.0791	1.128		1354.99	0.0792	1.102	
$^5F_5 \rightarrow ^5I_7$	995	453.81	0.0261	1.243		448.04	0.0260	1.211		444.139	0.0259	1.172	
$^5I_6 \rightarrow ^5I_8$	1032	209.41	0.0121	0.720		207.88	0.0121	0.705		206.501	0.0121	0.686	
$^5S_2 \rightarrow ^5I_5$	1195	239.68	0.0138	1.247		237.76	0.0138	1.215		235.968	0.0138	1.186	
$^5S_2 \rightarrow ^5I_6$	1310	63.85	0.0037	0.651		63.42	0.0037	0.636		63.007	0.0037	0.613	
$^5I_7 \rightarrow ^5I_8$	2035	95.21	0.0055	4.823		94.36	0.0055	4.716		93.665	0.0055	4.588	
$^5I_6 \rightarrow ^5I_7$	2925	24.28	0.0014	4.026		24.02	0.0014	3.921		23.814	0.0014	3.828	

V. CONCLUSION

In the present study, the glass samples of composition $(25-x)\text{P}_2\text{O}_5: 10\text{ZnO}: 10\text{Li}_2\text{O}: 10\text{K}_2\text{O}: 10\text{CaO}: 10\text{Al}_2\text{O}_3: 10\text{Yb}_2\text{O}_3: 15\text{B}_2\text{O}_3: x\text{Ho}_2\text{O}_3$. (where $x = 1, 1.5$ and $2\text{mol } \%$) have been prepared by melt-quenching method. The value of stimulated emission cross-section (σ_p) is found to be maximum for the transition ($5I_7 \rightarrow 5I_8$) for glass YZLPCABP (HO 01), suggesting that glass YZLPCABP (HO 01) is better compared to the other two glass systems YZLPCABP (HO1.5) and YZLPCABP (HO 02). The large stimulated emission cross section in tellurite glasses suggests the possibility of utilizing these systems as laser materials.

REFERENCES

- [1]. Mariselvam, K., L. Juncheng (2021). A Novel Tb³⁺ ions doped barium strontium fluorosilicate (Tb³⁺: BSFS) glasses for green laser emission and white LEDs. *Optik*, 233, 1-14.
- [2]. Kaur, R., Khanna, A. (2020). Photoluminescence and thermal properties of trivalent ion-doped lanthanum tellurite anti-glass composite samples, *Journal of Luminescence*, 225: 117375.
- [3]. Nasser, K., Aseev, V., Ivanov, S., Ignatiev, A. and Nikonorov, N. (2019). Optical spectroscopic properties and Judd-ofelt analysis of Nd³⁺ doped photo thermo refractive glass, *J. Lumin.* 213, 255-262.
- [4]. Chen, Y., Chen, G.H., Liu, X.Y. and Yang, T. (2018). Enhanced up-conversion luminescence and optical thermometry characteristics of Er³⁺/Yb³⁺ co-doped transparent phosphate Glass Ceramics, *Journal of luminescence* 195, 314-320.
- [5]. Monisha, M., Nancy, A., Souza, D., legde, V., Prabhu, N.S., Sayyed, M.I. (2020). Dy³⁺ doped SiO₂-B₂O₃-Al₂O₃-NaF-ZnF₂ glasses: An exploration of optical and gamma radiation shielding features, *Current Applied Physics* 20(11): 1207-1210.
- [6]. Reddy, A., Sekhar, M. C., Pradeesh, K., Babu, S. S., Prakash, G. V. (2011). Optical properties of Dy³⁺-doped sodium-aluminum phosphate glasses, *J Mater Sci.*, 46: 2018-2023.
- [7]. Hongisto, M., Vebar, A., Botti, N.G., Danto, S., Jubera, V. and Petita, L. (2020). Transparent Yb³⁺ doped phosphate glass ceramics, *Ceramics International* 46(16), 26317-26325.
- [8]. Wu, T., Cheng, Y., Zhong, H., Peng, H. and Hu, J. (2018). Thermal Stability and Spectral Properties of Tm³⁺, Yb³⁺ co-doped Tellurite Glasses. *Glass Phys. Chem.*, 44, 163-169.
- [9]. Vighnesh, K.R., Ramya, B., Nimitha, S., Wagh, A., Sayyed, M.I., Sakar, E., Yakout, H.A., Dahshan, A. (2020). Structural, optical, thermal, mechanical, morphological and radiation shielding parameters of Pr³⁺ doped ZAIFB glass systems, *optical materials*, 99: 109512.
- [10]. Chowdhury, S., Mandal, P., Ghosh, S. (2019). Structural properties of Er³⁺ doped lead zinc phosphate glasses *Mat. Sci. and Eng.*, 240, 116-120.
- [11]. Rao, V. R., Devi, L., Jayasankar, C.K., Pecharapa, W., Kaewkhao J. and Rani Depuru S. (2019). Luminescence and energy transfer studies of Ce³⁺/Dy³⁺ doped fluorophosphates glasses, *Journal of Luminescence*. 208, 89-98.
- [12]. Farag, M. A., Ibrahim, A., Hassaan M. Y. and Ramadan R.M. (2022). Enhancement of structural and optical properties of transparent sodium zinc phosphate glass-ceramics nano composite, *Journal of Australian Ceramic Society*. 58, 653-661.
- [13]. Sdiri, N., Elhouichet, H., Ferid, M. (2014). Effect of substituting P₂O₅ for B₂O₃ on the thermal and optical properties of sodium borophosphate glasses doped with Er, *J. Non-Cryst. Solids*, 389, 38-45.
- [14]. Thakur, S., Thakur, V., Kaur, A., Singh, L. (2019). Structural, optical and thermal properties of nickel doped bismuth borate glasses, *J. Non-Cryst. Solids*, 512, 60-71.
- [15]. Kolavekar, S.B., Ayachit, N.H. (2021). Impact of Pr₂O₃ on the physical and optical properties of multi-component borate glasses, *Mat. Chem. Phys.* 257, 1-10.
- [16]. Liu, L., Xing, J., Shang, F. and Chen, G. (2021). Structure and up-conversion luminescence of Yb³⁺/Ho³⁺ co-doped fluoroborate glasses. 490, 126944, 1-6.
- [17]. Kuwik, M., Kowalska, K., Pisarska, J., Pisarski, W.A. (2023). Spectroscopic Properties of Pr³⁺, Tm³⁺, and Ho³⁺ in Germanate-Based Glass Systems Modified by TiO₂, *Materials*, 16(61) 1-13.
- [18]. Mariselvam, K., Liu, J. (2021). Green emission and laser properties of Ho³⁺ doped titanate lead borate (TLB) glasses for colour display applications. *J. Solid State Chem.*, 293, 121793.
- [19]. Rani, P.R., Venkateswarlu, M., Swapna, K., Mahamuda, S.K., Srinivas Prasad, M.V.V.K., Rao, A.S. (2020). Spectroscopic and luminescence properties of Ho³⁺ ions doped Barium Lead Alumino Fluoro Borate glasses for green laser applications. *Solid State Sci.* 102, 106175.
- [20]. Meena, S.L. (2019). Spectral and Thermal Properties of Ho³⁺ doped oxy-fluoride glasses, *Int. J. Eng. Res. Mang.* 6, 1-8.



- [21]. Gorller-Walrand, C. and Binnemans, K. (1988). Spectral Intensities of f-f Transition. In: Gshneidner Jr., K.A. and Eyring, L., Eds., Handbook on the Physics and Chemistry of Rare Earths, Vol. 25, Chap. 167, North-Holland, Amsterdam, 101-264.
- [22]. Sharma, Y.K., Surana, S.S.L. and Singh, R.K. (2009) Spectroscopic Investigations and Luminescence Spectra of Sm³⁺ Doped Soda Lime Silicate Glasses. Journal of Rare Earths, 27, 773-780.
- [23]. Judd, B.R. (1962). Optical Absorption Intensities of Rare Earth Ions. Physical Review, 127, 750-761.
- [24]. Ofelt, G.S. (1962). Intensities of Crystal Spectra of Rare Earth Ions. The Journal of Chemical Physics, 37, 511.
- [25]. Sinha, S.P. (1983). Systematics and properties of lanthanides, Reidel, Dordrecht. 1-8.
- [26]. Krupke, W.F. (1974). IEEE J. Quantum Electron. QE, 10, 450.



INNO SPACE
SJIF Scientific Journal Impact Factor
Impact Factor: 8.423



ISSN INTERNATIONAL
STANDARD
SERIAL
NUMBER
INDIA



INTERNATIONAL JOURNAL OF INNOVATIVE RESEARCH

IN SCIENCE | ENGINEERING | TECHNOLOGY

9940 572 462 **6381 907 438** **ijirset@gmail.com**



www.ijirset.com

Scan to save the contact details